

## Numerical Analysis of Spray Coating Processes

Bamidele Olufemi Eyitope, Salaudeen Shakirudeen Alade,  
Mohamed Ifras Zubair, Araoye Abdulrazaq Adeniyi, Luai Al-Hadhrami  
Department of Mechanical Engineering, King Fahd University of Petroleum and Minerals,  
Dhahran 31261, Saudi Arabia

**Abstract:** This research work analyses the spray and impact regions of spray coating processes using Plane Laminar Jet and Stagnation Flow Models. In order to predict spray coating process behaviour, numerical simulations of fluid at the mentioned regions have been carried out using Mathematica and MATLAB commercial Packages. The models presented in this work can be used to predict an ideal orientation and condition of the solid and fluid phases for efficient spray coating, which minimizes material cost and reduces toxic emissions to the atmosphere. The present work would consequently bring about environmental sustainability.

**Keywords:** Numerical analysis, spray coating, laminar jet, stagnation flow, impact region, emissions.

### I. Introduction

Environmental and a reduced life cycle cost are important factors in industries today. Surface sustainability engineering is a valuable tool in achieving both of these, by facilitating optimal material selection and innovative product design. Sprays used for coating of materials like ships contains substances that are rated as hazardous air pollutants by EPA, such substances include xylene, toluene and methyl ethylketone. Overspray in coating processes also contains toxic particulates which can migrate with air, thereby causing contamination and damage to the environment[1].

In engineers' efforts to solve these abundant challenges in the industry, we find deposition processes such as, physical vapour deposition (PVD), chemical vapour deposition (CVD), anodizing, laser processing, thermal spraying, cold spraying, and liquid deposition methods.

These coating applications and performance characteristics are heavily dependent on the composition and processing parameters. More understanding of spray coating processes may help resolve environmental, safety and quality issues. These may be achieved via reduction in overspray and adherence to standard practice which help achieve more efficient surface coating.

Some applications of spray coating are, Auto-body shops, Sign painting, Furniture industries (such as doors), appliance manufacturing facilities, Metal fabrication and metal fabrication shops (where oilfield equipment, heavy machinery, and transportation equipment etc. are manufactured and repaired), as well as Sandblasting & coating facilities.

This research work investigates the fluid dynamics phenomena in spray coating process. It focused mainly on modelling the fluid behaviour at the spray region as well as the impact region, at the time of impact. The schematic of the present work (Figure 1) involves a stationary spray gun placed at a constant distance from the substrate. The substrate is at constant temperature and is moving perpendicularly to the spray gun. Only the fluid at the impact region i.e. the stagnation point is considered.

The objectives of this work are to:

- Numerically analyse flow field equations for spray and impact regions of a laminar flow jet.
- Numerically analyse energy equation for impact region of laminar flow jet.
- Interpret the resulting graphs and their practical applications in spray coating process.

Spray coating in fluid dynamics can be classified in three ways; the air blast atomization referred to as air spray painting, pressure atomization usually called airless spray painting and a combination of both[1]. Airless spraying uses a spray gun, where paint is forced through a very small orifice using hydraulic pressure. The main problem faced by this method is that the nozzles wear out faster, which also creates tails in the spray pattern, the movement of the hand gun is also restricted due to the high pressure (1000psi) in the hydraulic hoses. This method of spray coating typically has transfer efficiency within the range 20-30%, where 70-80% of the spray is released as harmful gases to the surrounding. In air-assisted airless type of spray coating, hydraulically formed spray film is atomized by the introduction of compressed air through orifices at the tip holder in the airless spray process, which helps to reduce wear and formation of spray pattern tails in the nozzle by reducing the hydraulic pressure.

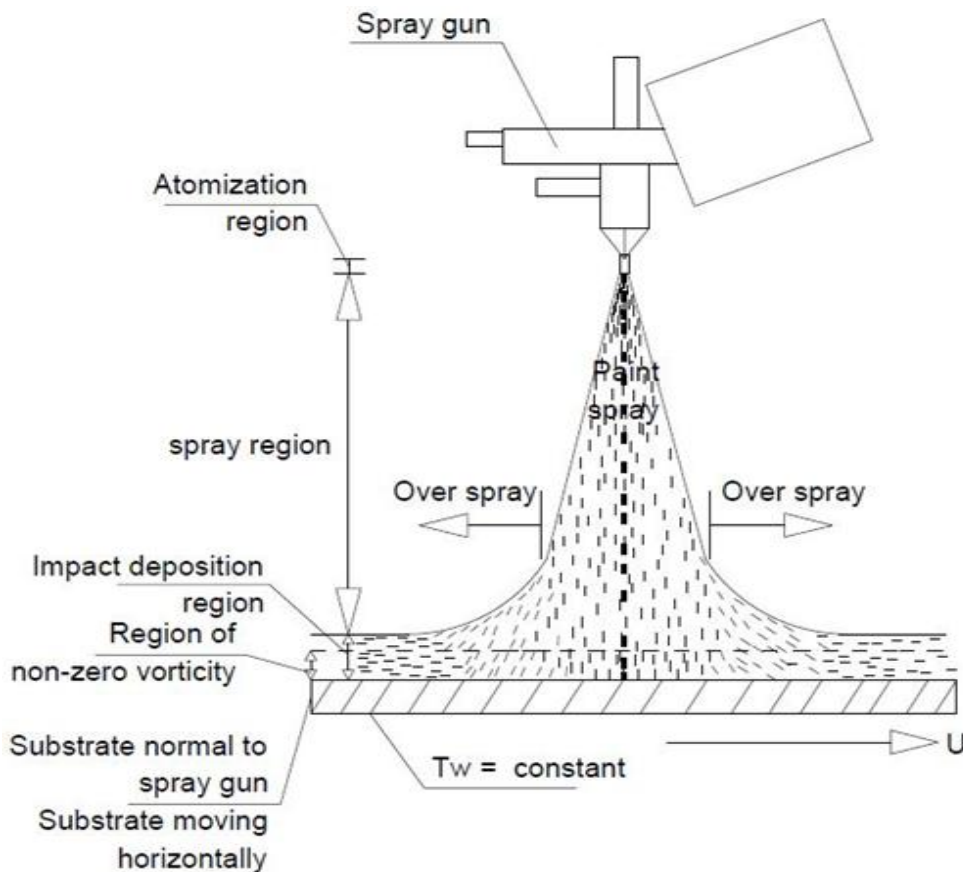


Figure 1: Schematic of Spray coating process

Generally, spray application is the preferred choice for achieving smooth finishes in a coating process, coating may also be applied using paint rollers, brushes etc.[2]. Added costs related to material waste, cleaning costs as well as harmful emissions released to the environment are major issues faced by many industries that use spray coating processes. An investigation by Tricou and Knasiak[3,4] showed that effervescent atomization techniques are capable of achieving high transfer efficiencies of around 95%.

B. Andersson[4] categorized droplet breakup into two; Primary and secondary breakups. Typically, fragments break before reaching a stable size, which is known as the secondary breakup sometimes referred to as spray region. This is to some extent independent of the primary one, as droplets continue to break until they are stable. During droplet breakup, surface tension acts at the air-liquid interface as a stabilizing force to prevent further breakup. Surface tension acts with a magnitude that is proportional to the mean curvature of the interface; it is therefore crucial to have control over the interface. The spray region splits spray particles into a large particle segment which strikes the target, and a small-particle segment which does not[4]. The number of droplets produced after breakup is sensitive to the location of the impact point on the substrate [5]. The fraction that is not likely to strike the target is highly probable to become overspray. The discrimination of large & small particles is characterized by a Stokes number, which compares the aerodynamic response time of the particle to a time scale associated with the structure of the flow. The overspray generally spreads into the surrounding atmosphere. The planar wall jet is known to grow linearly in thickness with distance from the impingement point, and eventually to separate from the wall[1].

An important property of spray is the viscosity or consistency of spray. This determines the amount of wet film that may be applied[2]. Increase in spray viscosity results in thicker strands that require a higher gas flow rate to split the jets into droplets[6]. In turn, when the coating is thinned (dilute or less viscous), atomization is easier; however, this changes the speed of drying which could result in many consequences. Excessive thinning also creates problems such as blushing in the final coating results. Also, the higher the spray pressure, the better the atomization of the jet, however, this may lead to material waste due to overspray [2].

Air volume and material volume are two important factors affecting spray atomization. Insufficient air flow leads to improper atomization, which will be seen on the surfaces spots of liquid. Excessively low material volume results in a weak spray stream and causes delays in applying the finish. Conversely, excessively high material volume, illustrates problems with inadequacy of air volume as this would result in an attempt to

atomize greater proportion liquid in comparison to the volume of air flowing through the gun. Increment in both material and air volume, will enable the spray gun reach its maximum capacity relative to the coverable surface area per unit time. These factors may be tweaked to attain the best results[2]. A study illustrating the effects of gas-to-liquid ratio (GLR) with respect to drop thickness on typical liquids showed that at the low viscosity range, a hump in the droplet Mass Mean Diameter (MMD) response could be found in very low GLR range[6]. This increase in MMD in conventional spraying is due to strands that form during liquid sheet disintegration. This condition can be corrected through the addition of a small amount of gas. An increment of GLR causes the strand diameter and spacing to decrease, it also produces smaller droplets[6].

Besides fluid properties, the spray gun is a key component in a finishing system. Spray guns are classified based on their modes of atomization[7]. Every spray nozzle constructed has its respective application and particular range of flow, in order to produce a preferred drop size and velocity distribution. The flow rate depends on the nozzle area, geometry, the feed pressure and the nature of the fluid. For a fixed nozzle, a higher flow rate leads to larger droplet sizes, whereas higher gas flow leads to smaller droplet sizes.

Another important parameter of the spray gun is the fan width. It controls the level of roundness of the spray stream. A wide spray pattern is preferred since it covers a larger area making the spray process quicker. Too wide fan will lead to the droplets of liquid not flowing together, which results in a clustered surface known as "orange peel". On the other hand, inadequate fan width requires extra passes to conceal the region being sprayed, which often results in additional runs and sags. A heavier coat gives slow travel, and fast travel provides a lighter coat. Theoretically, a lumpy appearance could be created if the travel rate is too fast since droplets may be too far apart to mix together. However, in comparison a travel rate too fast causes fewer problems than moving too slowly[2].

Detailed understanding of the differences between systems lead to the selection of the precise gun required in order to produce a high quality finish and contribute towards less costly finishing operations [2]. The above conclusions are further supported by the work of Huang et al [8] on the effects of differences in atomizer designs using computational fluid dynamics (CFD).

Several research works have been done on numerical analysis of spray coating process. An analysis of the mechanism of spray deposition by means of computational fluid dynamics (CFD) performed by Fogliati et al [9] presumed that the initial droplet velocities and liquid jet velocity at the moment of breakage were the same. A preliminary simulation was performed to estimate the thinning before the occurrence of breakage of the liquid jet in the region local to the nozzle. The method was validated through comparison with experimental data by phase Doppler anemometry and, subsequently, the approach was applied to spray deposition, to different geometries and operating conditions (normal wall, wall at 60 degree, 45 degree and also to an edge). A research by Domnick and Khalifa[10] using experimental and numerical modelling showed that the initial conditions necessary for the simulations of the droplets could be taken close to the nozzle. By the application of practically relevant air and spray flow parameters, the resulting film thickness distribution calculated using FLUENT commercial code, corresponded with the experimental data.

An approach to constructing a size distribution and a velocity profile would be to construct a bivariate probability density function, which is the key for a moments-based spray model.[11]. Ayres et al [12], developed a mathematical model to forecast the size and velocity of droplets in sprays, based on the maximum entropy formalism. Using measurable parameters, the authors made correlations for the average velocity of the air blast atomizers as well as that of pressure jet based on assumed profiles in the atomizer gun. They further predicted several distributions for various types of atomizers. The developed model by the authors would be useful to engineers designing atomizers, and would also help prevent the use of complex measurement programs to find the initial conditions for spray flow calculations.

According to Mahesh and Sojka[13], the maximum velocity of an effervescent spray occurs along the centreline of the spray. Jet velocity decreases with an increase in distance from the nozzle exit. The jet flow rate has negligible effect on changes in drop size [13]. Dilute spray radial droplet velocity varied with axial distance relative to the free gas jets.

Accurate simulations of spray and drop transfer efficiencies over the range of drop diameters, produced by the atomizer can be obtained when the direct effects of air turbulence are accounted for with a stochastic separated flow formulation[14]. Drop transfer efficiency of larger spray droplets is higher than smaller droplets because of the large inertia effect due to their momentum. In contrast, deposition of smaller drops is far less efficient, and was shown to be controlled by the nature of the turbulent air flow field[14].

## **II. Mathematical Modeling**

This work focuses on laminar spray jet for spray coating process. Modelling of fluid behaviour at the spray and impact region, at the time of impact have been considered.

Initial conditions and assumptions shall be:

- Flow is assumed to be laminar, steady, plane, two dimensional, viscous and incompressible. Assuming constant temperature within the spray region and on the substrate.
- Spray Jet is considered as a control volume.
- The atomizer is stationary, whereas the substrate is moving.
- Substrate is normal to atomizer. Substrate is moving horizontally (as shown in figure 1).
- Distance between the atomizer and substrate is fixed.
- Ambient air during impact of droplet is assumed to be dynamically inactive. i.e only liquid phase is considered.
- Tangential stresses for the free surface are neglected.
- No slip, no temperature jumps between the impact fluid and the substrate.
- The spray nozzle tip used within this problem is assumed to be rectangular with a thin film exit.
- Only spray at centerline velocity (stagnation point) deposits on the substrate.

Three of the conservation equations of fluid flow have been employed in this study, which are:

- i. The continuity equation.
- ii. The Momentum (Navier-Stokes) equation.
- iii. The Energy equation.

The spray region has been treated using The Plane Laminar Jet model, while the Impact Region has been analysed using Hiemenz Flow model and Goldstein Energy Model.

A numerical analysis of the resulting flow field equation of the spray region has been carried out using Mathematica, while simulation of the Impact Region has been done using Matlab.

Two out of the three regions shown in figure 1 are treated below. They are;

- a) The Spray Region
- b) The Impact Region

The spray region has been treated with the use of laminar jet model with the assumption of constant temperature of the fluid within the spray region while the impact region has been treated using stagnation flow model; Heimenz solution and Goldstein solution have been adopted for the momentum and fluid energy balance at the stagnation point respectively[15], while C.Y Wang solution [16] has been adopted to cater for the moving substrate.

### **The Spray Region**

Considering the spray as a plane jet emerging into a still ambient air from a nozzle at  $y=0$ , as shown in figure 2. There is no bounding wall around the spray jet therefore;

- i. The jet spreads at atmospheric (constant) pressure.
- ii. The jet has constant momentum flux, vertically down the stream across any distance  $y$ . where 'y = constant'

$$\text{Continuity: } \frac{\partial u}{\partial x} + \frac{\partial v}{\partial y} = 0 \tag{1}$$

$$\text{Y - Momentum: } u \frac{\partial v}{\partial x} + v \frac{\partial v}{\partial y} = \vartheta \frac{\partial^2 v}{\partial x^2} \tag{2}$$

Momentum Flux:

$$J = \rho \int_{-\infty}^{+\infty} v^2 dx = \text{constant} \tag{3}$$

$$u = \frac{\partial \psi}{\partial y} \tag{4}$$

$$v = -\frac{\partial \psi}{\partial x} \tag{5}$$

The Stream function

$$\psi = \vartheta^{\frac{1}{2}} y^{\frac{2}{3}} \beta(\eta) \tag{6}$$

Where

$$\eta = \frac{x}{3\vartheta^{\frac{1}{2}} y^{\frac{2}{3}}} \tag{7}$$

$$v = \frac{\beta'(\eta)}{3y^{\frac{1}{3}}} \tag{8}$$

$$u = -\frac{\vartheta^{\frac{1}{2}}(\beta - 2\beta' \eta)}{3y^{\frac{2}{3}}} \tag{9}$$

Then, from equations (1 & 2)

$$\beta''' + \beta\beta'' + \beta'^2 = 0 \tag{10}$$

With the boundary conditions of when  $x = 0, u = 0$  and  $\frac{\partial v}{\partial y} = 0$  and at  $x = \infty, v = 0$

Applying these conditions to the similarity variables, will give:

$$\beta(0) = \beta'(\infty) = 0 \text{ and } \beta'(\infty) = 0$$

$$\beta(\eta) = 2a \tanh(a\eta)$$

$$\beta'(\eta) = 2a^2 \operatorname{sech}^2(a\eta)$$

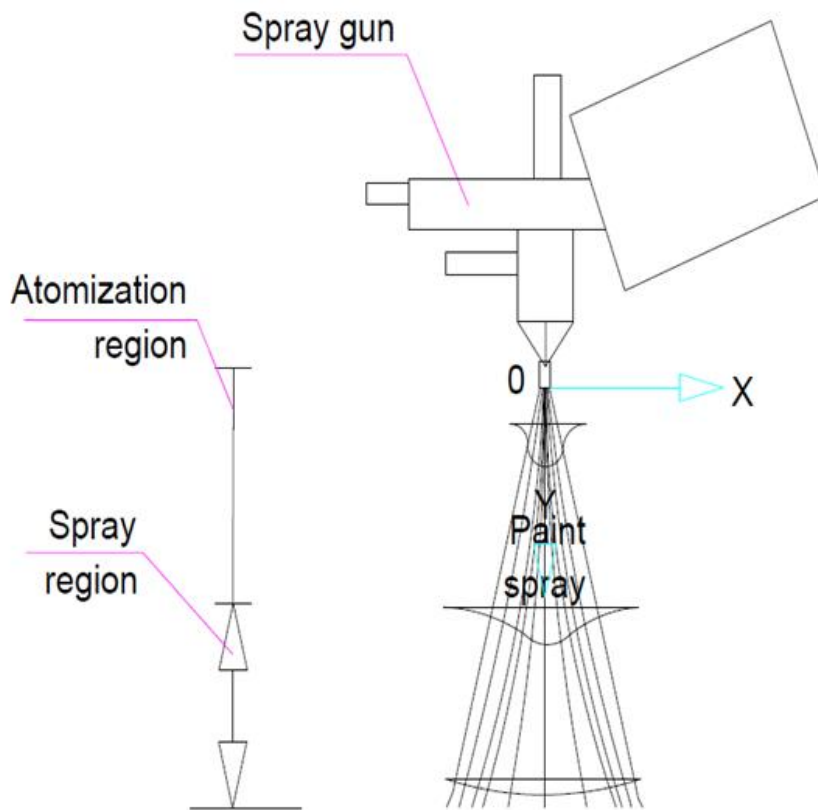


Figure 2: Schematic Illustrating Laminar Planar Jet

$$J = \rho \int_{-\infty}^{+\infty} \left( \frac{2a^2}{3y^3} \operatorname{sech}^2 a\eta \right)^2 * 3\vartheta^{\frac{1}{2}} y^{\frac{2}{3}} d\eta = \frac{16}{9} \rho \vartheta^{\frac{1}{2}} a^3 \quad (11)$$

$$a = \left( \frac{9J}{16\sqrt{\rho\mu}} \right)^{\frac{1}{3}} = 0.8255 * \frac{J^{\frac{1}{3}}}{(\rho\mu)^{\frac{1}{6}}} \quad (12)$$

with,  $\operatorname{sech} 0 = 1$ ,

$$v_{max} = \frac{2a^2}{3y^3} = \frac{2}{3} \left( \frac{9}{16} \right)^{\frac{2}{3}} * \frac{J^{\frac{2}{3}}}{(\rho\mu y)^3} \approx 0.4543 \left( \frac{J^2}{\rho\mu y} \right)^{\frac{1}{3}} \quad (13)$$

Thus the jet spreads so that the maximum velocity drops off as  $y^{-\frac{1}{3}}$ . The velocity distribution is:

$$v(x, y) = v_{max} \operatorname{sech}^2 a\eta = v_{max} \operatorname{sech}^2 \left[ 0.2752 \left( \frac{J\rho}{\mu^2 y^2} \right)^{\frac{1}{3}} * x \right] \quad (14)$$

We may define the width of the jet as twice the distance  $x$  where,  $v = 0.01v_{max}$ , and noting that  $\operatorname{sech}^2 3 \approx 0.01$ , we have;

$$width = 2x|_{1\%} = b \approx 21.8 \left( \frac{y^2 \mu^2}{J\rho} \right)^{\frac{1}{3}} \quad (15)$$

So, the jet spreads as  $y^{\frac{2}{3}}$ . The mass flow rate across any vertical plane is given by:

$$\dot{m} = \rho \int_{-\infty}^{+\infty} u dx = (36J\rho\mu y)^{\frac{1}{3}} \approx 3.302(J\rho\mu y)^{\frac{1}{3}} \quad (16)$$

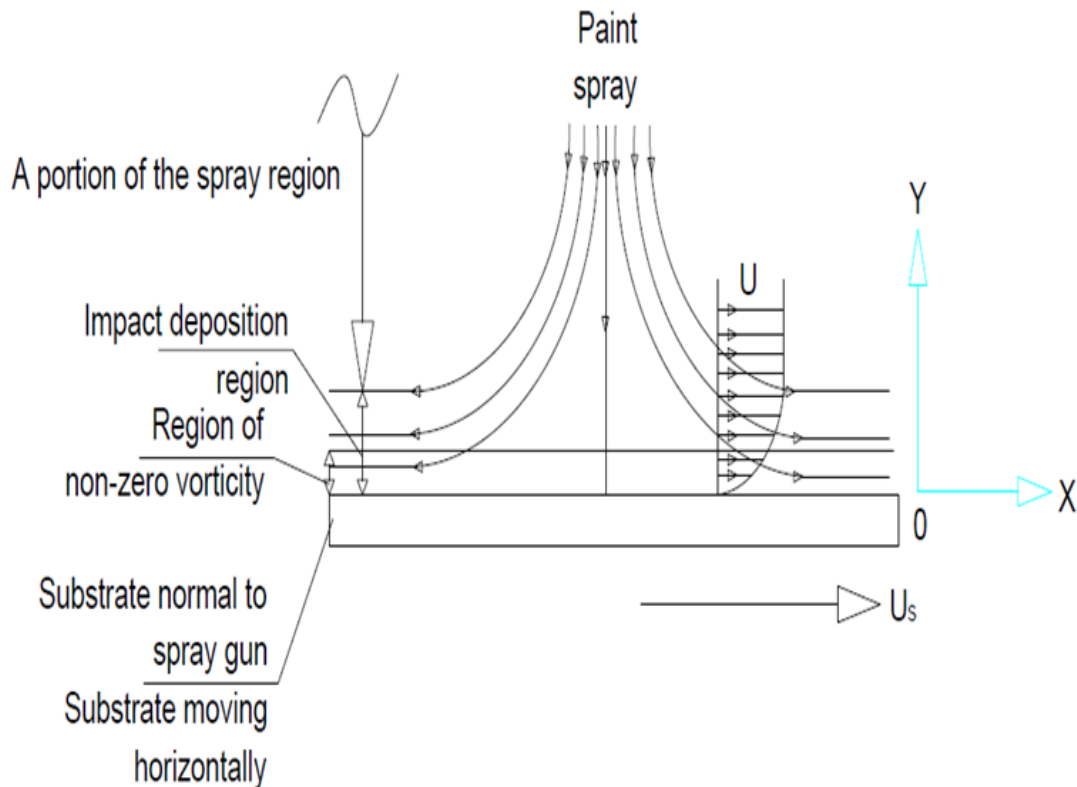


Figure 3: Schematics of Stream Lines of Paint Spray Approaching the Impact Region

**Hiemenz Similarity Solution (For a Stationary Substrate)**

Continuity;  $\frac{\partial u}{\partial x} + \frac{\partial v}{\partial y} = 0$  (17)

*x* – Momentum;  $u \frac{\partial u}{\partial x} + v \frac{\partial u}{\partial y} = \frac{-1}{\rho} \frac{\partial p}{\partial x} + \nu \left( \frac{\partial^2 u}{\partial x^2} + \frac{\partial^2 u}{\partial y^2} \right)$  (18)

*y* – Momentum;  $u \frac{\partial v}{\partial x} + v \frac{\partial v}{\partial y} = \frac{-1}{\rho} \frac{\partial p}{\partial y} + \nu \left( \frac{\partial^2 v}{\partial x^2} + \frac{\partial^2 v}{\partial y^2} \right)$  (19)

Let stream function:

$\psi_{viscous} = Bxr(y)$  (20)

where  $r(y)$  accounts for viscous effects.

$u = \frac{\partial \psi}{\partial y} = Bxr'$  (21)

$v = -\frac{\partial \psi}{\partial x} = -Br(y)$  (22)

For the no slip condition at the wall,

$u|_{y=0} = U_s$ , (23)

$r'(0) = 0$  (24)

$v|_{y=0} = 0$ , (25)

$r(0) = 0$  (26)

Bernoulli's equation,

$P_o = P + \frac{\rho}{2} (u^2 + v^2)$  (27)

$\frac{P_o - P}{\rho} = \frac{1}{2} ((Bxr')^2 + (-Br)^2)$  (28)

$P_o - P = \frac{\rho B^2}{2} (x^2 + r(y))$  (29)

$\therefore \frac{-1}{\rho} \frac{\partial p}{\partial x} = B^2 x$ , and  $\frac{-1}{\rho} \frac{\partial p}{\partial y} = \frac{B^2 r'}{2}$  (30)

$v = -r(y)$

For Viscous flow;

since,  $v = -r(y)$

$\therefore \frac{\partial v}{\partial x} = \frac{\partial^2 v}{\partial x^2} = 0$ ;  $\frac{\partial v}{\partial y} = -r'$ ,  $\frac{\partial^2 v}{\partial y^2} = -r''$  (31)

since,  $u = xr'$

$$\therefore \frac{\partial u}{\partial x} = r', \frac{\partial^2 u}{\partial x^2} = 0; \frac{\partial u}{\partial y} = xr'', \frac{\partial^2 v}{\partial y^2} = r''' \quad (32)$$

$$-\frac{1}{\rho} \frac{\partial p}{\partial x} = B^2 x \text{ and } -\frac{1}{\rho} \frac{\partial p}{\partial y} = \frac{B^2}{2} r' \quad (33)$$

Substituting into the Navier Stokes equation,

$$xr' r' r'^2 - rr'' = B^2 + \vartheta r''' \quad x - \text{momentum}; \quad (34)$$

$$y - \text{momentum};$$

$$rr' = \frac{B^2}{2} r' - \vartheta r'' \quad (35)$$

**Boundary Conditions;**

At  $y=0 \rightarrow u = v = 0$  and  $P = P_0$

At  $y = 0 \rightarrow r = r' = 0 \quad (36)$

At  $y = \infty, u = U = Bx$  (solution approaching inviscid flow)

$$\frac{du}{dx} = r' = B \quad (37)$$

From similarity variables,

$$\eta = y \sqrt{\frac{B}{\vartheta}}, \quad \varphi = \frac{1}{\sqrt{B\vartheta}} r \quad (38)$$

$$\frac{d\eta}{dy} = \sqrt{\frac{B}{\vartheta}}, \quad \frac{dy}{d\eta} = \sqrt{\frac{\vartheta}{B}} \quad (39)$$

$$\varphi' = \frac{r}{B' \sqrt{\vartheta}} \quad (40)$$

$$\varphi'' = \frac{r' \sqrt{\vartheta}}{(\sqrt{B})^3} \quad (41)$$

$$\varphi''' = \frac{r'' \vartheta}{B^2} \quad (42)$$

Substituting equations (40 – 42) into equation (35);

$$\varphi''' + \varphi'' \varphi - \varphi'^2 + 1 = 0 \quad (43)$$

**Heimenz Similarity Solution Modification for a Moving Substrate**

Let the Cartesian velocity components at infinity be  $u = Bx, v = By$  which represents a potential axisymmetric stagnation flow. Let the plate be at  $y = 0$ , moving with constant velocity  $U$  in the  $x$  direction.. In order to cater for the velocity of the moving substrate, according to Wang C. Y. (1973)[16], there is a need to provide for a velocity term in the equation. Let;

$$u = U_x(\eta) + \chi B \varphi'(\eta) \quad (44)$$

$$v = -2\sqrt{B\vartheta} \varphi(\eta) \quad (45)$$

$$\eta = \sqrt{B/\vartheta} z \quad (46)$$

Substituting equations (44 - 46) into Navier Stokes equation:

$$\varphi''' + \varphi \varphi'' - (\varphi')^2 + 1 = 0 \quad (47)$$

$$\chi'' + \chi \chi' - \chi \varphi' = 0 \quad (48)$$

**Boundary Conditions:**

$$\varphi(0) = \varphi'(0) = 0, \varphi'(\infty) = 1 \quad (49)$$

$$\chi(0) = 1, \chi(\infty) = 0 \quad (50)$$

**Goldstein energy profile for stagnation point flow**

Goldstein established that for a similarity solution to exist for stagnation flow, the wall and ambient temperature have to be constant [15]. He also established that at stagnation point flow is independent of the

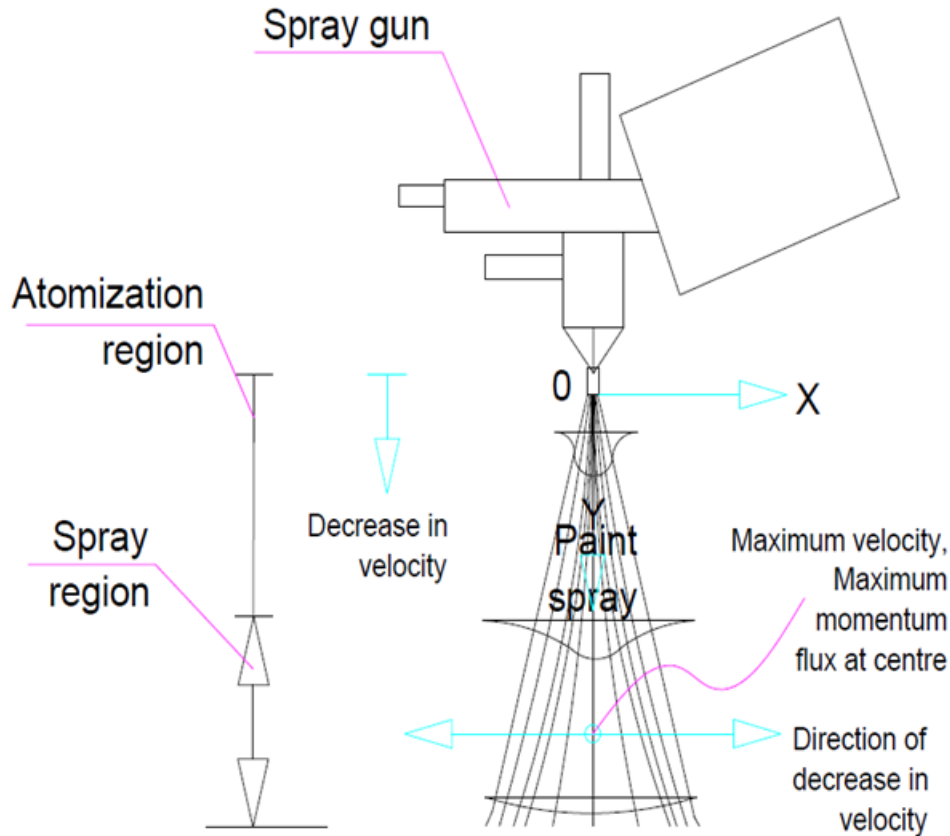


Figure 4: Schematics Illustrating Jet Behaviour in Spray Region Laminar Planar Jet

distance along the plate/substrate. For this work however, a situation of constant wall temperature over the substrate length is being considered with an assumption of constant temperature at a particular time of impact at the stagnation point. The governing energy equation is as stated below:

Energy equation;

$$u \frac{\partial T}{\partial x} + v \frac{\partial T}{\partial y} = \alpha \frac{\partial^2 T}{\partial y^2} \quad (51)$$

From similarity variables,  $\theta(\eta) = \frac{T-T_w}{T_\infty-T_w}$  and  $\eta = y \sqrt{\frac{U_\infty}{\nu x}}$  (52)

$$\frac{\partial T}{\partial x} = \theta' (T_\infty - T_w) \left( \frac{-\eta}{2x} \right) \quad (53)$$

$$\frac{\partial T}{\partial y} = \theta' (T_\infty - T_w) \sqrt{\frac{U_\infty}{\nu x}} \quad (54)$$

$$\frac{\partial^2 T}{\partial y^2} = \theta'' (T_\infty - T_w) \left( \frac{U_\infty}{\nu x} \right) \quad (55)$$

Applying stream function:

$$\varphi = f(\sqrt{U_\infty \nu x}); \quad (56)$$

$$u = \frac{\partial \varphi}{\partial y}, \quad v = -\frac{\partial \varphi}{\partial x} \quad (57)$$

$$u = U_\infty f' \quad (58)$$

$$v = -\frac{\partial \varphi}{\partial x} \quad (59)$$

Substituting equations (53, 54, 55, 58 & 59) into equation (51)

$$\theta'(-\eta U_\infty f' + \eta U_\infty f'' - U_\infty f) = \alpha \theta'' \frac{U_\infty}{\nu} \quad (60)$$

$$\theta'' + Pr f \theta' = 0 \quad (61)$$

**Boundary Conditions:**

$$y = 0, T = T_w, \theta(0) = 0; \quad y \rightarrow \infty, T = T_\infty, \theta(\infty) = 1 \quad (62)$$

Re-writing the coupled linearized ODE's (equations 42, 47 & 60) for Numerical solution, let:

$$\begin{aligned} x_1 &= \varphi, \quad x_2 = \varphi', \quad x_3 = \varphi'', \quad x_4 = \chi, \\ x_5 &= \chi', \quad x_6 = \theta, \quad x_7 = \theta' \\ x_1 &= x_2 \end{aligned} \quad (63)$$

$$x_2' = x_3 \tag{65}$$

$$x_3 = -2x_1x_3 + (x_2)^2 - 1 \tag{66}$$

$$x_4 = x_5 \tag{67}$$

$$x_5 = -2x_1x_5 + x_4x_2 \tag{68}$$

$$x_6 = x_7 \tag{69}$$

$$x_7 = -Prx_1x_7 \tag{70}$$

Equations (63 - 70) have been solved using Wolfram Mathematica commercial package and MATLAB commercial package.

**Discussion of Results for classified flow regions**

*Laminar flow jet region*

Consider the spray as a plane jet emerging into a still ambient air from a nozzle at  $y = 0$  as in Figure 2. It is assumed that there is no bounding wall around the spray jet, which implies that the jet spreads at constant pressure (atmospheric) and has constant momentum flux, vertically down as it approaches the substrate along any streamline, where the distance  $y$  between the gun and the substrate is constant.

From Equation 16, the mass flow is not a function of 'x', it is therefore constant down the stream. At any particular value of 'x' (from the centre line), from the equation above, the maximum velocity and momentum flux would be at the centre line (at  $y = 0, \eta = 0$ ), being that the horizontal component of the jet velocity is zero,  $\beta'(\eta) = 2a^2$ . This max velocity reduces towards the edges of the spray region as the flow moves away from the centre line.

From the plot of  $\frac{u}{U}$  against  $\eta(x, y)$  Figure 9, it is reflected that down the stream (as the jet approaches the substrate), the velocity of the jet reduces. This (the jet) will get to a point where the velocity will eventually die down. Also from the plot it is seen that it will take shorter distance for flow with higher  $\frac{u}{U}$  to die down than it will take flow of lower value of  $\frac{u}{U}$ . In order for the flow to reach the substrate, the plate should be placed at a minimum of this distance by considering the value of  $\frac{u}{U}$  before the velocity dies down

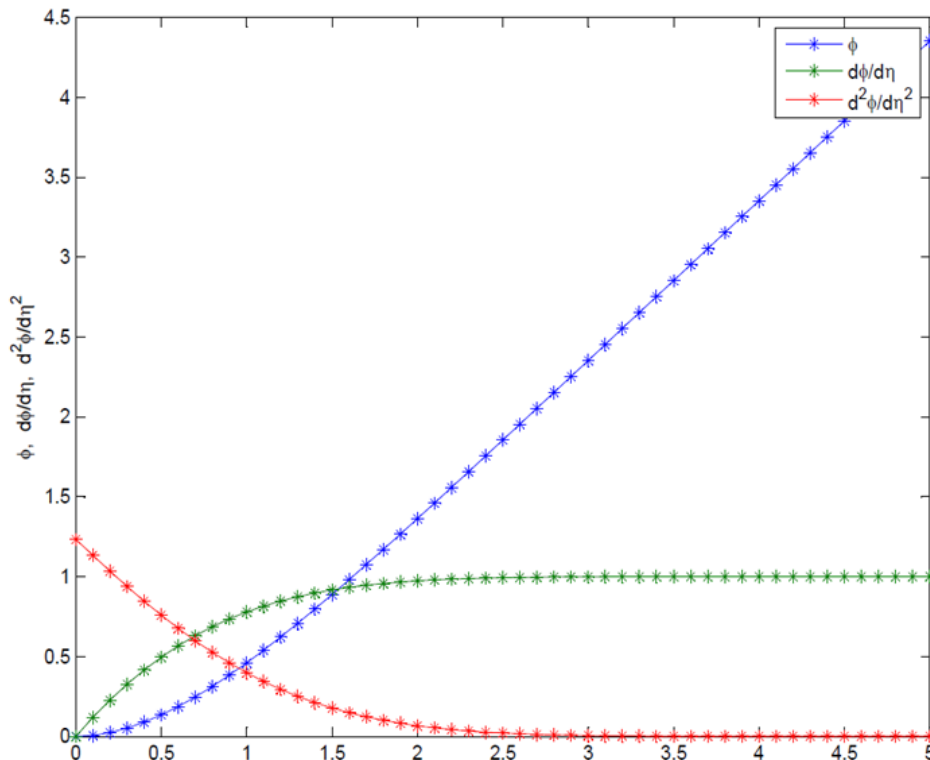


Figure 5: Validation of Hiemenz Similarity Solution for a Stationary Substrate

**III. Results of fluid flow in Impact region**

Figure 5, represents plot of stream function, velocity and shear stress against distance above the substrate ( $\eta$ ) for a substrate at stagnation point. From these plots, at the surface of the substrate ( $\eta = 0$ ), the shear stress is of order of 1.25 units due to fluid flow above the plate. This eventually dies down at a distance in the order of 2.7

units above the plate. On the surface of the substrate ( $\eta = 0$ ), the velocity of the fluid = 0 because it assumes the velocity of the plate, which is stationary. Farther above the substrate, at a distance in the order of 2.4 units, the velocity of the fluid above the plate will equals 0.999 of the free stream velocity. This is the boundary layer thickness of the fluid flowing above the substrate.

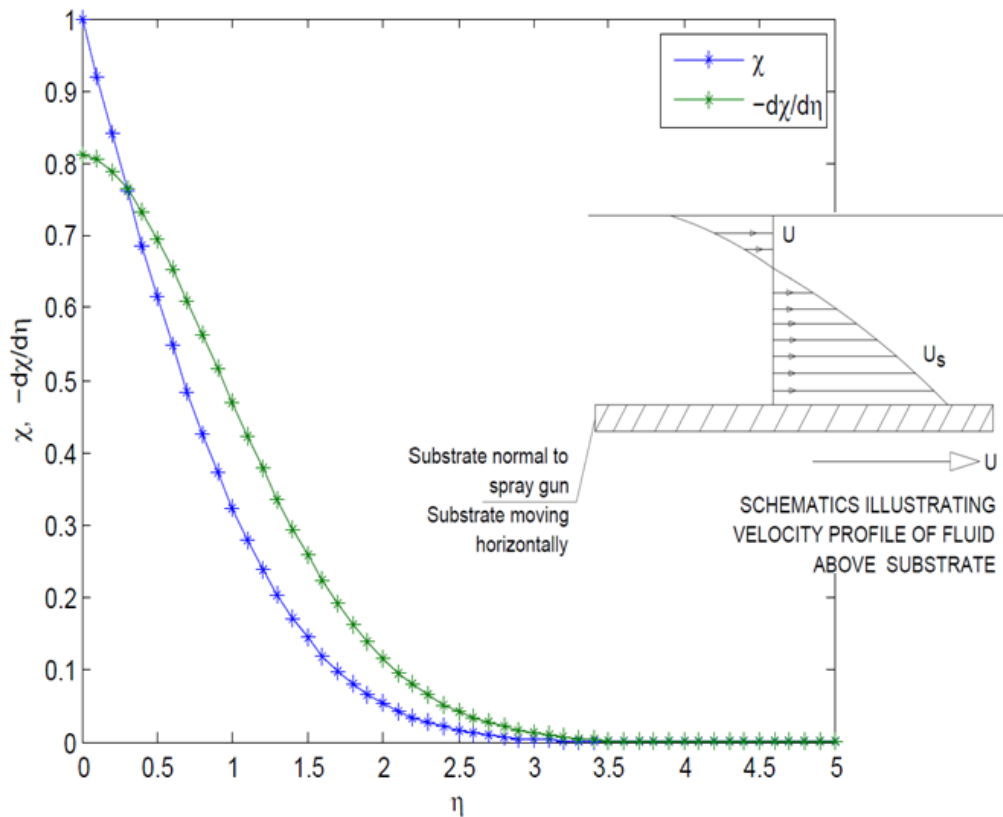


Figure 6: Plot of Modified Hiemenz Flow for a Moving Substrate

Figure 6 represents plot of velocity and negative shear stress against the distance above the moving substrate ( $\eta$ ). On the substrate ( $\eta = 0$ ), the fluid will assume the velocity of the substrate, which is of the order 1.0 unit. Farther above the substrate, at a distance  $\eta = 3.5$ , then the velocity of the fluid will be equals 0.999 of the free stream velocity. It is also shown from the figure that on the surface of the substrate, the shear stress is of the order -0.8113 units, the value of the shear stress increases as the distance above the plate increases.

*Results of temperature profile at stagnation point*

Fig 7 describes the temperature profile for different prandtl numbers similar to Goldstein solution.  $\theta$  in the above graph is related to the temperature of the wall, the ambient temperature and the fluid temperature.  $\eta$  is related to the distance from the substrate. In validating the energy model with Goldsteins stagnation point temperature profile, the Prandtl number was varied from 0.01 to 10. Prandtl number ( $Pr < 1$ ) represents fluids with larger thermal boundary layers and significantly smaller compared to the viscous layer. Therefore, if such fluids are used as sprays, heat is transferred within the fluid layer faster than the momentum. The opposite case applies for fluids with  $Pr > 1$ .

Fig 8 presents the temperature distribution within the fluid layer at the stagnation point. The fluid considered is water at 28°C (301K) ambient temperature, Prandtl number 5.68, wall temperature at stagnation point is 60°C (333K) and substrate is at 2 unit distance from the gun. It can be seen from the plot that the fluid layer that is directly in contact with the substrate (at  $y = 0$ ) assumes the temperature of the substrate 60°C (333K), and as we proceed within the thin film of water upwards towards the ambient air, the temperature reduces to a point where it is about 99% of the ambient temperature (when  $y = 1.1 \times 10^3$ ) which is the thermal Boundary Layer thickness and eventually reaches the ambient temperature 28°C (301K) after which it remained constant.

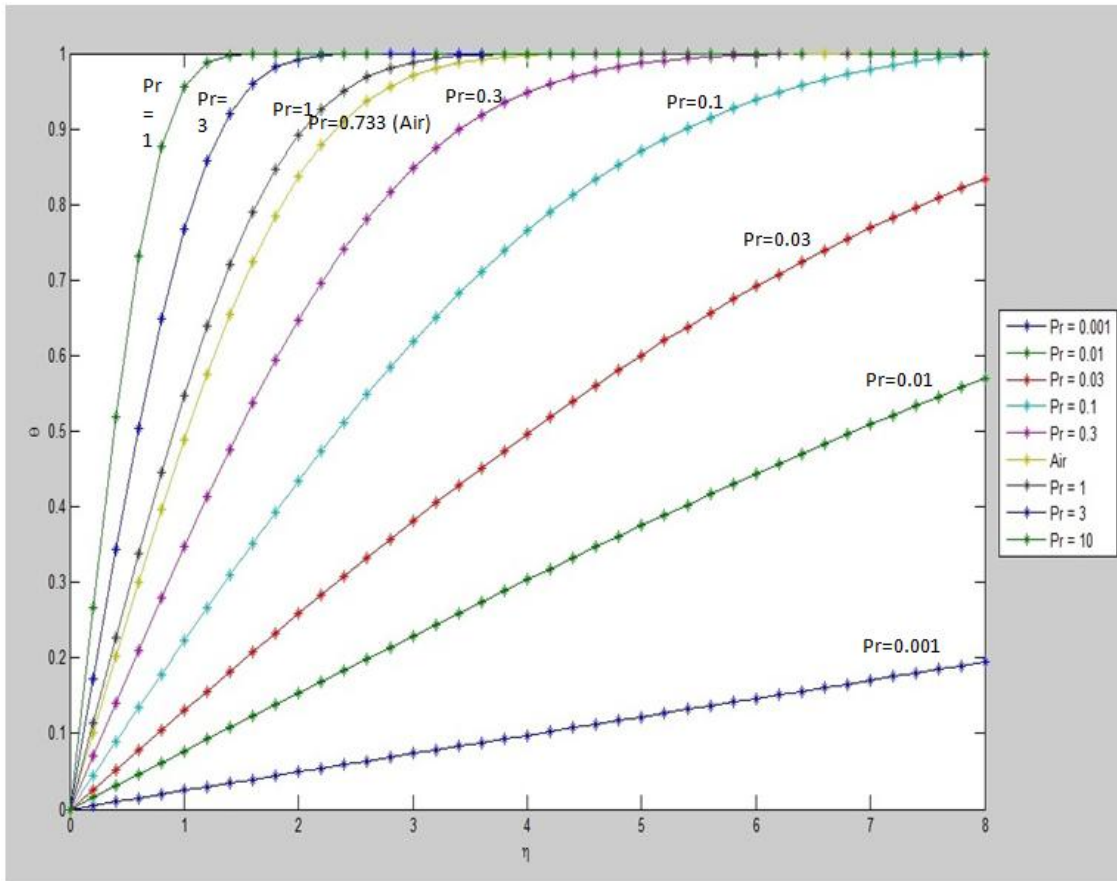


Figure 7: Validation of Goldstein Temperature Profile

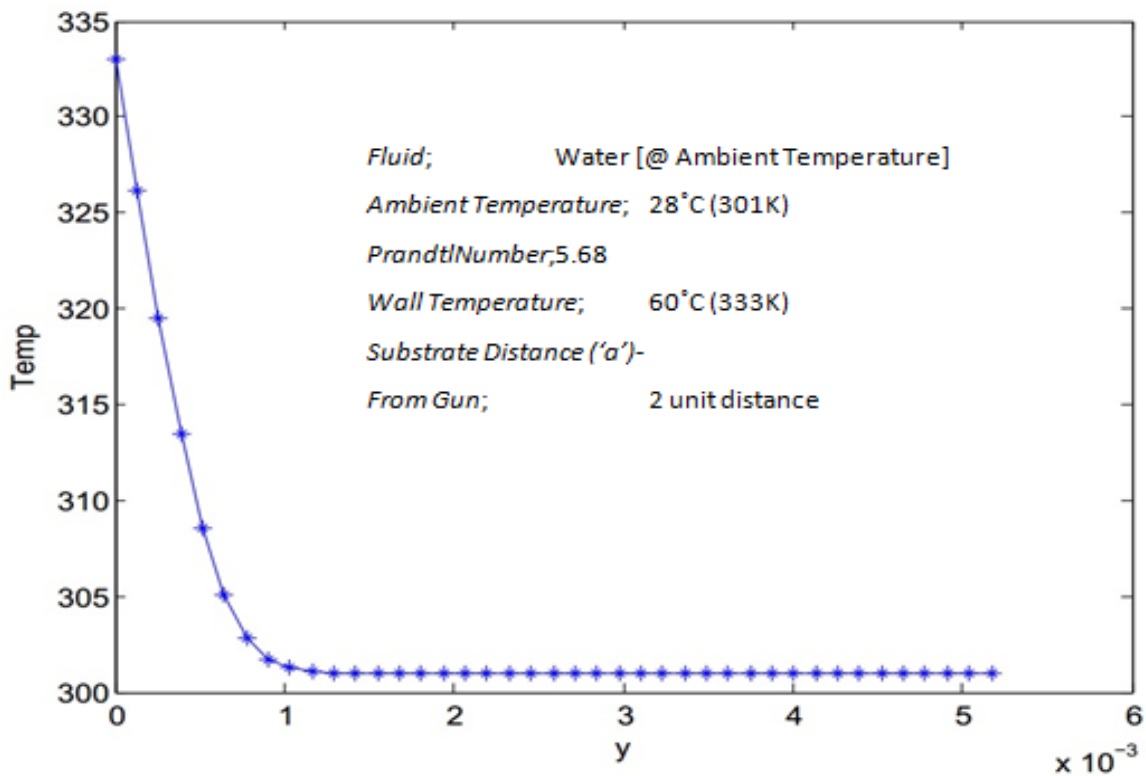


Figure 8: Temperature distribution within fluid layer at stagnation point.

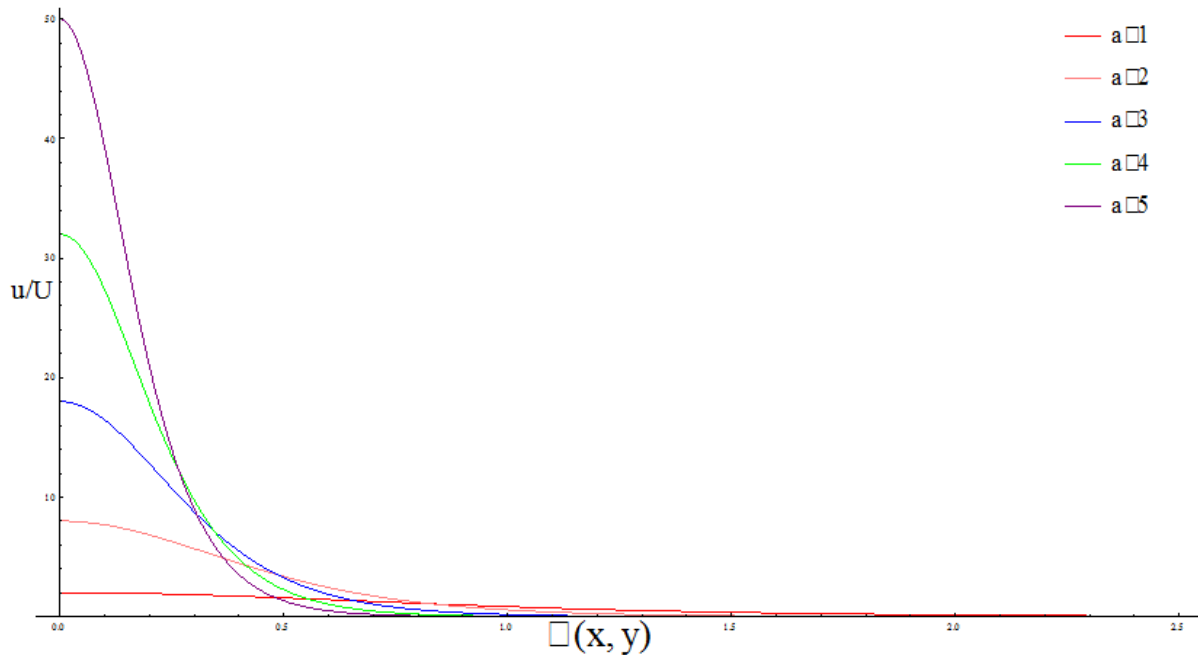


Figure 9: Resulting Graph of Spray Region Numerical Analysis

#### IV. Conclusion

Achieving an efficient simulation of painting/coating process is of paramount importance in manufacturing industry, because it helps to predict the efficiency of any given proposed process before the actual implementation of the process. This help to reduce waste of material and down time.

Applications in areas such as Auto-body shops, Sign painting, Furniture industries (such as doors), appliance manufacturing facilities, Metal fabrication and metal fabrication shops (where oilfield equipment, heavy machinery, and transportation equipment etc. are manufactured and repaired), as well as Sandblasting & coating facilities, will be well optimized and waste to the environment shall be reduced to a minimum under the present understanding.

Besides material cost, economic cost is of prior importance. Environmental cost is a more benign quantity, but is of great importance. In the case of paint overspray, being responsible suggests better efficiencies since efficient systems also mean less pollutants.

#### Acknowledgments

The authors would like to thank King Fahd University of Petroleum and Minerals in Dhahran, Saudi Arabia for funding this research.

#### NOMENCLATURE

$J$  Fluid momentum flux ( $\text{kg/m-s}^2$ )

$m$  Mass of fluid (kg)

$P$  Pressure ( $\text{N/m}^2$ )

$Pr$  Prandtl number

$T$  Temperature (C)

$u$  Fluid velocity component in x direction (m/s)

$v$  Fluid velocity component in y direction (m/s)

#### Dimensionless Functions

$r$  Dimensionless function to account for fluid viscosity

$\beta$  Dimensionless function to account for fluid momentum in spray region

$\phi$  Dimensionless function to account for fluid momentum in impact region

$\chi$  Dimensionless function to account for substrate velocity

#### Greek letters

$\eta$  Similarity variable for momentum

$\Theta$  Similarity variable for momentum ( $\text{m}^{-1}$ )

$\mu$  Dynamic viscosity of the fluid ( $\text{kg/m-s}$ )

$\nu$  Kinematic viscosity of the fluid ( $\text{m}^2/\text{s}$ )

$\rho$  Density of the fluid ( $\text{kg/m}^3$ )

$\psi$  Stream function

**Constants**

a

B

**Subscripts and Superscripts**

$o$  Initial property condition

$\infty$  Free stream

w Substrate

$x$  Horizontal component

$y$  Vertical component

' Differential sign

**REFERENCES**

- [1] G. S. Settles, "A Flow Visualization Study of Airless Spray Painting," in 10th Annual Conference on Liquid Atomization and Spray Systems, 1997, pp. 145–149. (Proceedings)
- [2] Parex USA, "Metallic Coating Using Conventional & HVLP Spray Guns," Parex USA Coatings, 2013. (Report)
- [3] Kwok, Hui-chiu, and B. Y. H. Liu, "How atomization affects transfer efficiency," *Ind. Finish.*, vol. 28, 1992. (Journal Article)
- [4] B. Andersson, "Droplet Breakup in Automotive Spray Painting," 2011. (Report)
- [5] M. Pasandideh-Fard, M. Bussmann, S. Chandra, and J. Mostaghimi, "SIMULATING DROPLET IMPACT ON A SUBSTRATE OF ARBITRARY SHAPE," *At. Sprays*, vol. 11, pp. 397–414, 2001. (Journal Article)
- [6] D. Loebker and H. J. Empie, "Effervescent Spraying," in TAPPI Engineering Conference, 1998. (Proceedings)
- [7] C. Fu, P. E. Sojka, and Y. R. Sivathanu, "On The Interaction Between Evaporating Sprays and Heated Surfaces," in Proceedings of the 12th Annual Conference on Liquid Atomization and Spray Systems, Indianapolis, IN, 1989. (Proceedings)
- [8] L. X. Huang, K. Kumar, and a. S. Mujumdar, "A comparative study of a spray dryer with rotary disc atomizer and pressure nozzle using computational fluid dynamic simulations," *Chem. Eng. Process. Process Intensif.*, vol. 45, no. 6, pp. 461–470, Jun. 2006. (Journal Article)
- [9] M. Fogliati, D. Fontana, M. Garbero, M. Vanni, and G. B. Politecnico, "CFD Simulation of Paint Deposition In an Air Spray Process," vol. 3, no. 2, pp. 117–125, 2006. (Journal Article)
- [10] Q. Ye, J. Domnick, and E. Khalifa, "SIMULATION OF THE SPRAY COATING PROCESS USING A PNEUMATIC ATOMIZER," in ILASS-Europe 2002, 2002, no. September. (Proceedings)
- [11] D. P. Jones and a. P. Watkins, "Droplet size and velocity distributions for spray modelling," *J. Comput. Phys.*, vol. 231, no. 2, pp. 676–692, Jan. 2012. (Journal Article)
- [12] D. Ayres, M. Caldas, V. Semiao, and M. da GracaCarvalho, "Prediction of the droplet size and velocity joint distribution for sprays," *Fuel*, vol. 80, pp. 383–394, 2001. (Journal Article)
- [13] M. V. Panchagnula and P. E. Sojka, "Spatial droplet velocity and size profiles in effervescent atomizer-produced sprays," *Fuel*, vol. 78, no. 6, pp. 729–741, May 1999. (Journal Article)
- [14] P. G. Hicks and D. W. Senser, "Simulation of Paint Transfer in an Air Spray Process," *J. Fluids Eng.*, vol. 117, pp. 713–719, 1995. (Journal Article)
- [15] F. M. White, *Viscous Fluid Flow*. 2006, pp. 144–153, 253–255. (Book)
- [16] C.-Y. Wang, "Axisymmetric stagnation flow towards a moving plate," *AIChE J.*, vol. 19, no. 5, pp. 1080–1081, Sep. 1973. (Journal Article)